GaAs:$Cr^{3+}(3d^3)$—an orthorhombic Jahn-Teller center with a stress-dependent reorientation rate

G. H. Stauss and J. J. Krebs
Naval Research Laboratory, Washington, D.C. 20375
(Received 31 March 1980)

The $Cr^{3+}(3d^3)$ EPR center in GaAs has been investigated using controlled uniaxial stress at temperatures from 1.8 to 4.2 K. Stresses up to 1200 kg/cm^2 were applied along the [001], [111], [110], and [112] axes. The rapidity of stress alignment of the distortions at 1.8 K shows that the orthorhombic symmetry arises from a Jahn-Teller (JT) effect. At high stress levels, the populations of the favored distortions behave as expected for a static JT effect. As the stress is reduced to low levels, however, the signal amplitudes decrease anomalously while the linewidths increase. Simultaneously, the lines develop Lorentzian tails and shift somewhat in position, and even at 1.8 K there is no microwave saturation. This behavior suggests a rapid reorientation between nearly equivalent distortions at low (or zero) applied stress which is quenched at high stress. The single-phonon-induced reorientation rate is shown to be stress dependent and can give rise to line broadening (fast reorientation) at low stress. A model based on this and a Boltzmann distribution over the different distortions gives semiquantitative agreement with the normalized signal amplitudes from the energetically favored distortions. The data show that the center couples strongly to both E and T_2 modes and the Jahn-Teller coupling coefficients are determined. The E and T_2 couplings are nearly equal in the sense of O'Brien and this is responsible for the fast low-temperature reorientation ($\tau \simeq 0.3$ ns at 1.8 K). For $\vec{P} \parallel [001]$ an observed P/T scaling of the data and a splitting of the 4-kG EPR line at low stress remain unexplained.

INTRODUCTION

In an earlier publication,[1] we reported the first EPR observation of $Cr^{3+}(3d^3)$ in a III–V semiconductor and noted that the Cr^{3+} center in GaAs has a number of unusual properties. These include: (1) orthorhombic symmetry (C_{2v}) even though Cr is apparently substitutional for Ga which has cubic (T_d) site symmetry, (2) a rapid decrease in observability of the spectrum when the temperature is raised above 5 K, and (3) a sensitivity of both the *absolute* signal amplitudes and the *relative* signals from differently oriented centers to the rather poorly defined sample-mounting stress. These properties were attributed[1] to a strong Jahn-Teller effect in which the Cr^{3+} center (including its four ligands) rapidly reorients between the six equivalent orthorhombic distortions. Each center has principal axes along a cube edge and its two orthogonal face diagonals.

We have now examined the Cr^{3+} center under conditions of controlled uniaxial stress, and it is the purpose of this paper to demonstrate more clearly the nature of the Jahn-Teller distortion. We shall show that the six equivalent distortions represent well-defined vibronic energy minima resulting from the combined effect of both E and T_2 symmetry distortion modes on the center. Even at 1.8 K, reorientation between different distortions is so rapid in the absence of applied stress that the Cr^{3+} center can be considered essentially "dynamic" on the time scale of the EPR experiment. By means of applied stress we are able to induce a dynamic-to-static Jahn-Teller transition. This is due to the increasing localization of the center wave function as stress makes the various distortions energetically inequivalent. To our knowledge this is the first observation of such a transition. The data establish Cr^{3+} in GaAs as a very clear-cut example of a Jahn-Teller center with orthorhombic minima. Some aspects of the observed behavior are not fully explained, however.

We first give the theoretical background necessary to understand the origins of the unusual Jahn-Teller behavior. After a brief description of the techniques used, the experimental observations are then described in detail. Next, these results are discussed in relation to the theoretical ideas developed earlier and, finally, we draw conclusions about the Cr^{3+} center.

THEORETICAL BACKGROUND

In order to discuss the Jahn-Teller effect[2] and the possibility of orthorhombic distortion of an orbital triplet state T_1 (or T_2), we will follow the treatment of Bacci *et al.*[3] In a system possessing only linear electron-lattice coupling and harmonic elastic behavior, the Hamiltonian suitable to the $^4T_1$ ground state of Cr^{3+} in a tetrahedral cubic site will be written as

$$\mathcal{H} = -aQ_A \mathcal{I} - (2b/\sqrt{3})(Q_\theta \mathcal{E}_\theta + Q_\epsilon \mathcal{E}_\epsilon) - c(Q_{xy}\mathcal{T}_{xy} + Q_{yz}\mathcal{T}_{yz} + Q_{zx}\mathcal{T}_{zx}) + [\tfrac{1}{2}\kappa_A Q_A^2 + \tfrac{1}{2}\kappa_E(Q_\theta^2 + Q_\epsilon^2) + \tfrac{1}{2}\kappa_T(Q_{xy}^2 + Q_{yz}^2 + Q_{zx}^2)]\mathcal{I}. \quad (1)$$

Here $\mathcal{I}$, $\mathcal{E}_\theta$, $\mathcal{E}_\epsilon$, $\mathcal{T}_{xy}$, $\mathcal{T}_{yz}$, and $\mathcal{T}_{zx}$ are 3×3 matrix operators[2] based on the triplet of electronic states, the Q's are vibrational modes of A_1, E, or T_2 symmetry, a, b, and c are the electron-lattice-coupling coefficients, and the κ's are effective elastic constants. Several approximations are inherent in this formulation. Spin-orbit interactions are neglected, and the vibronic wave functions are taken as simple Born-Oppenheimer product functions in which the electronic and displacement coordinates are separated. Symmetry modes suitable to a molecular cluster are assumed, and only one of the two possible sets of T_2 modes of distortion is taken to be significant.

For an arbitrary normalized electronic-state vector $\vec{a} = (\alpha, \beta, \gamma)$ spanning T_1 or T_2, which can be expressed in spherical coordinates as $(\sin\theta\cos\varphi, \sin\theta\sin\varphi, \cos\theta)$, the corresponding equilibrium energy E_a can be evaluated by minimizing the quantity $\langle a|\mathcal{H}|a\rangle$ with respect to the various Q's. With $\mathcal{H}$ in the form of Eq. (1) this results in

$$E_a = -\left(\frac{1}{2}\frac{a^2}{\kappa_A} + \frac{2}{3}\frac{b^2}{\kappa_E}\right) + 2\left(\frac{b^2}{\kappa_E} - \frac{c^2}{\kappa_T}\right)(\alpha^2\beta^2 + \beta^2\gamma^2 + \gamma^2\alpha^2) \equiv V_0 + V_1(\alpha^2\beta^2 + \beta^2\gamma^2 + \gamma^2\alpha^2). \quad (2)$$

Written in the latter form, this expression is entirely analogous to the lowest-order expression for cubic magnetic anisotropy energy. An immediate consequence of Eq. (2) is that for $V_1 = 0$ the energy is entirely independent of the choice of electronic state within T_1 or T_2. In this special case all vectors $\vec{a}$ constitute stationary states of the Hamiltonian.[4] For nonzero V_1 only state vectors of the types (111), (110), and (001) constitute stationary states, with energies $V_0 + V_1/3$, $V_0 + V_1/4$, and V_0. Since these three cases correspond to equilibrium distortions having, respectively, trigonal, orthorhombic, and tetragonal symmetry, the well-known result appears that for a T_1 or T_2 state in the *linear* Jahn-Teller regime a static orthorhombic distortion is never favored energetically.[5]

With the addition of nonlinear Jahn-Teller–coupling terms and anharmonic elastic terms to the Hamiltonian of Eq. (1) this situation is changed, as discussed by Bacci *et al.*[3] The various possible terms added, suitably chosen to preserve cubic symmetry, have the effect of modifying V_0 and V_1 while introducing a higher-order anisotropy $V_2\alpha^2\beta^2\gamma^2$ in Eq. (2) so that

$$E_a = V_0 + V_1(\alpha^2\beta^2 + \beta^2\gamma^2 + \gamma^2\alpha^2) + V_2\alpha^2\beta^2\gamma^2. \quad (3)$$

The possible new terms[3] are too many to allow individual identification here, but the influence of the V_2 term they produce can easily be described. Depending on the values of V_1 and V_2, not only tetragonal and trigonal but now also orthorhombic distortions can fall lowest in energy. Such orthorhombic distortions introduce the new feature of simultaneously coupling the center to E and T_2 distortions. When the orthorhombic distortion is favored, the smallest barrier between equivalent minima is defined by the existence of a saddle point on the E_a surface. To stabilize the orthorhombic distortion it is necessary that $V_1 < 0$ and $V_2 > \frac{9}{4}|V_1|$. The saddle point then lies at an energy $-\frac{1}{4}V_1(1 + 2V_1/V_2)^2$ above the minimum.

We presume that the higher-order contributions are relatively small. Hence the conditions for orthorhombic distortion are most readily satisfied when the "linear" contribution to V_1 is small. This suggests that near equality should exist between b^2/κ_E and c^2/κ_T, and that the barrier be low. Under such conditions, anticipating also that the isotropic contribution is relatively small, a reasonable approximation to the Jahn-Teller energy becomes

$$E_{JT} \simeq -\frac{2}{3}\frac{b^2}{\kappa_E}. \quad (4)$$

The isotropic mode is not entirely insignificant, however, since in higher-order terms it can contribute to V_1 and V_2.

A typical orthorhombic distortion is the one having nonzero values of Q_A, Q_θ, and Q_{xy} only. To lowest order their equilibrium values are a/κ_A, $b/\sqrt{3}\kappa_E$, and $-c/\kappa_T$, respectively. Also to lowest order, with the Q's fixed at these ground-state values, the excited electronic states have energies $(b^2/\kappa_E) + (c^2/\kappa_T)$ and $2c^2/\kappa_T$ above the ground state. Near $V_1 = 0$ these excited states should be almost degenerate except for the influence of higher-order terms.

When external stress is applied to the system the equilibrium energy of a distorted center will change. Since the stress effects will be small, they can be treated to lowest order as simply establishing new elastic equilibrium positions with respect to which the distortions occur (cf. Appendix of Ref. 2). The only changes in energy will then be due to strains belonging to the same symmetries as the Jahn-Teller distortions. For the typical center having only Q_A, Q_θ, and Q_{xy} distortions, the change in energy becomes

$$\Delta E_a = -a\Delta_A - (b/\sqrt{3})\Delta_\theta + c\Delta_{xy}, \quad (5)$$

TABLE I. Equivalent orthorhombic distortions.

Type	Principal axes [a] x	z	Reduced local-stress components [b] for $\vec{P}\|\|$ [001] $\hat{e}_\theta$	[111] $\hat{e}_{xy}$	[110] $(\hat{e}_\theta, \hat{e}_{xy})$	[112] $(\hat{e}_\theta, \hat{e}_{xy})$	Field for Cr^{3+} resonance $\vec{H}_0$ (kOe) $\|\|$ [1$\bar{1}$0]
1	[011]	[100]	$-\frac{1}{2}$	$\frac{1}{3}$	$\frac{1}{4}, 0$	$-\frac{1}{4}, \frac{1}{3}$	1.7
2	[0$\bar{1}$1]	[$\bar{1}$00]	$-\frac{1}{2}$	$-\frac{1}{3}$	$\frac{1}{4}, 0$	$-\frac{1}{4}, -\frac{1}{3}$	1.7
3	[101]	[010]	$-\frac{1}{2}$	$\frac{1}{3}$	$\frac{1}{4}, 0$	$-\frac{1}{4}, \frac{1}{3}$	1.7
4	[10$\bar{1}$]	[0$\bar{1}$0]	$-\frac{1}{2}$	$-\frac{1}{3}$	$\frac{1}{4}, 0$	$-\frac{1}{4}, -\frac{1}{3}$	1.7
5	[110]	[001]	1	$\frac{1}{3}$	$-\frac{1}{2}, \frac{1}{2}$	$\frac{1}{2}, \frac{1}{6}$	2.8
6	[$\bar{1}$10]	[00$\bar{1}$]	1	$-\frac{1}{3}$	$-\frac{1}{2}, -\frac{1}{2}$	$\frac{1}{2}, -\frac{1}{6}$	4.0

[a] $g_x < g_y < g_z$.
[b] The strain e_θ in units of $P(s_{11} - s_{12})$, e_{xy} in units of Ps_{44}. P is negative in compression.

where Δ_A, Δ_θ, and Δ_{xy} are the changes in the equilibrium $\mathcal{Q}$'s due to stress. Higher-order terms in the Hamiltonian will of course modify the coefficients of the Δ's and introduce higher powers of the Δ's as well.

The main significance of Eq. (5) is that for different directions of stress, or equivalently for a fixed stress applied to centers having differently oriented distortion axes, the values of Δ_θ and Δ_{xy} (but not of Δ_A) will vary. For each of the six possible orthorhombic distortions, Table I shows the geometrical factors $\hat{e}_i$ which are proportional to Δ_θ and Δ_{xy} measured in the local x, y, z axes for the different directions of stress used in our work. The strains e_i induced by a stress of magnitude P are given by $e_\theta = P(s_{11} - s_{12})\hat{e}_\theta$ and $e_{xy} = Ps_{44}\hat{e}_{xy}$, where the s_{ij} are the elastic moduli. The Δ_i quantities can then be obtained[6] from $\Delta_i = f_i e_i$ where $f_\theta = f_{xy}/\sqrt{3} = (2\sqrt{2}/3)R_{NN} = a_0/\sqrt{6}$ (R_{NN} is nearest-neighbor distance, a_0 the lattice constant). The strain e_θ is defined as $\frac{1}{2}(2e_{zz} - e_{xx} - e_{yy})$ in the local system. As a consequence of Eq. (5), the various distortions will become inequivalent in energy for a general stress, resulting in a Boltzmann distribution favoring the lowest-energy state.

The discussion above has all presupposed that the six orthorhombic states represent static distortions. However, in principle one knows that the initial undistorted T_1 state is only threefold degenerate. Furthermore, the vibronic wave functions of the orthorhombic stationary states are not orthogonal except in pairs. Hence in the absence of low-symmetry perturbations the true eigenstates of the Hamiltonian will be linear combinations of the individual static distortion states. This situation is quite different from the tetragonal E-mode distorted system found[7] for Cr^{2+} in GaAs where the distortion modes are disjoint.

The orthorhombic case is analogous to the one-dimensional systems discussed by Sussmann.[8] Tunneling due to overlap between wave functions of equivalent minima will result in mixed states whose properties will be quite distinct from those of a static distortion. One can obtain some insight into the nature of the true eigenstates by considering the form of the tunneling matrix between the equivalent static orthorhombic states. From symmetry it has the form[9]

$$\begin{pmatrix} 0 & 0 & t & t & t & -t \\ 0 & 0 & -t & -t & t & -t \\ t & -t & 0 & 0 & t & t \\ t & -t & 0 & 0 & -t & -t \\ t & t & t & -t & 0 & 0 \\ -t & -t & t & -t & 0 & 0 \end{pmatrix},$$

where the matrix elements between two states which have the same cube edge as a principal axis vanish and the signs of the other off-diagonal elements depend on the choice of relative phase for the basis states. Independent of this choice there are two triply degenerate eigenstates (Ref. 9), T_1 at the energy $-2t$ and T_2 at $2t$. In this situation, of course, one would not observe any EPR from orthorhombic centers.

With the introduction of perturbations which make individual orthorhombic distortions energetically inequivalent, the nature of the true eigenstates will change. Any states which become nondegenerate will rapidly assume the character of pure static distortions as the energy separations increase. Those states which remain degenerate, however, can be expected to continue to mix. During this transition from a dynamic to a static situation, one can anticipate that resonance parameters of the lowest-lying state of the system will show some variation, and that the lifetime of that state will increase as the admixture decreases. The general

TABLE II. Samples used.

Stress axis	Total Cr^{3+} (10^{15})	Other dopants	Source
[001]	0.34		NRL
[111]	0.56	Sn	NRL
[110]	1.37	Mn	HP
[110]	0.68	Te	NRL
[112]	1.49		Monsanto

criterion[2] for the existence of a static Jahn-Teller effect is that the perturbation-produced energy differences between different distortions exceed the tunneling splitting, $4t$. It is still possible for transitions between "static" states to occur via various phonon-assisted processes at rates dependent on temperature, the energy splitting, and the strength of the tunnel coupling (i.e., the barrier height).[8] Hence whether one observes the static distortion or not depends on whether the transition rate is sufficiently slow on the time scale of the experiment. This fact plays an important role in understanding the GaAs:Cr($3d^3$) system.

EXPERIMENTAL METHOD AND RESULTS

The EPR-stress apparatus used for these experiments has been described earlier.[7] It permits 100-kHz-modulated x-band EPR measurements in the 1.8- to 4.2-K temperature range while uniaxial stress P is applied to the sample. Modulation amplitudes were limited to 5 Oe p.-p. by eddy-current boiling of the liquid helium in which the cavity and sample are immersed, despite a series of circumferential slits in the cavity plating. Data were taken mainly at 1.8 K and also at 4.2 K. It also proved practicable to obtain a series of intermediate-temperature data of reasonable validity during the warmup following cessation of pumping on the cryostat.

The five samples identified in Table II were investigated. The samples were cut as rectangular solids with lengths from 10 to 15 mm and cross-sectional areas from 1.6 to 4.7 mm^2. The long, x-ray-aligned stress axes are given in Table II. The maximum stress applied was 1200 kg/cm^2.

In general we found that in the absence of stress, even at 1.8 K, only very weak Cr^{3+} EPR signals can be observed. Our previously reported signals resulted from the presence of complex mounting stresses in the samples. Under conditions of strong controlled stress and lower temperatures, the signals become considerably stronger than we were able to observe before. Even at relatively low stress levels the signals which appear (except for rather small position shifts as a function of stress) are defined by the parameters reported earlier.[1] Hence our efforts were mainly directed to examining the effects of stress on the signals obtained with the applied magnetic field along high-symmetry directions where the signals are strongest and best defined. For all five samples, $\vec{H} \parallel [1\bar{1}0]$ could be achieved and only data for this orientation will be presented. For the applied field along $[1\bar{1}0]$, four of the six possible distortion orientations are magnetically equivalent. These yield a resonance at about 1.7 kOe, while the other two give resonances near 2.8 and 4.0 kOe (see Table I and cf. Fig. 3 of Ref. 1). The effect of stress is to enhance certain of these lines and to weaken or eliminate others. Stresses change the linewidths and slightly alter line positions, particularly at low stress levels. These effects will now be described in detail.

Stress ∥ [001]

This is the stress orientation examined in the most detail, partly because of favorable signals. The variation in the $\vec{H} \parallel [1\bar{1}0]$ peak-to-peak signal amplitude with stress at 1.8 K is shown in Fig. 1. In the absence of applied stress on this sample the three resonance lines are essentially unobservable. Note that the signal at 1.7 kOe never appears. The linewidths of the two observable signals behave as shown by the inset in Fig. 1. The shapes of these lines also change with stress, developing irregularities, significantly greater widths, and longer tails at low stress.

In Fig. 2 similar amplitude and linewidth data for

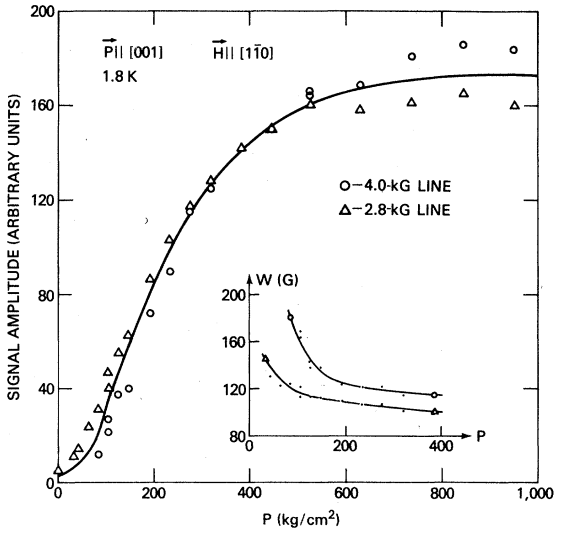

FIG. 1. Stress dependence of derivative signal *amplitudes* observable with $\vec{P} \parallel [001]$, $\vec{H} \parallel [1\bar{1}0]$ at 1.8 K. Insert shows corresponding p.-p. linewidths. Solids curves are aids to the eye only.

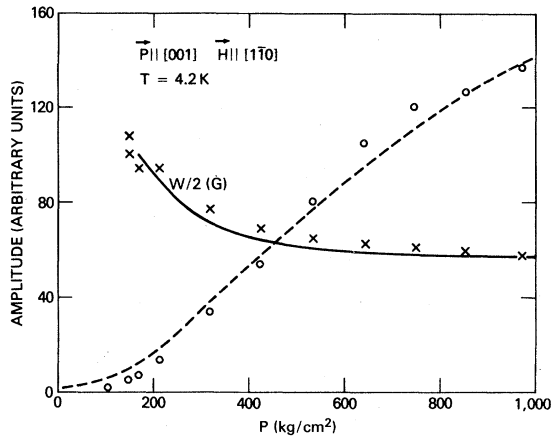

FIG. 2. Stress dependence of the amplitude (mean of 2.8- and 4-kG lines) and width (4-kG line only) for $\vec{P} \parallel [001]$, $\vec{H} \parallel [1\bar{1}0]$ but at 4.2 K. Dashed and solid curves are corresponding data from Fig. 1 scaled as P/T (see text). The 2.8-kG width data are affected by background distortion.

4.2 K are shown. Again no 1.7-kOe signal was found. The variation of the amplitudes of the 2.8-kOe and 4.0-kOe signals as a function of temperature is seen in Fig. 3. These last data were taken at a constant stress of 256 kg/cm^2 and are less precise than those shown in the other figures since the temperature was changing continuously as the cryostat warmed up over a period of about 30 min.

A particularly interesting point which arises from the stress and temperature data is that except for thermal population changes among the electronic-spin states of a center, the signal amplitudes depend only on the ratio P/T to a good approximation. For example, comparison of Figs. 1 and 2 shows that a much larger stress is required at 4.2 K than at 1.8 K before significant 2.8- and 4.0-kOe signals appear. If, however, the average data of Fig. 1 are corrected for the spin level population differences between 1.8 and 4.2 K and for the small microwave saturation at high stress, then those data give the dashed curve in Fig. 2 when the applied stress is scaled as P/T. The solid curve in Fig. 2 is the corresponding linewidth data from Fig. 1 again employing P/T scaling. A further test of this scaling is shown in Fig. 3 where the temperature-dependent amplitude data are compared with the P/T-scaled 1.8-K data indicated by the solid line. In each case there is rather good agreement between the data at higher temperatures and the scaled 1.8-K data even though no arbitrary factor is introduced in the scaling procedure.

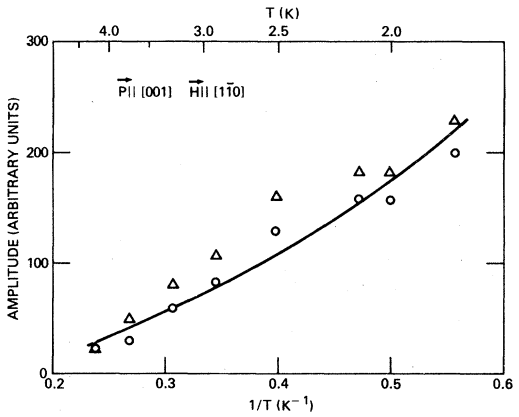

FIG. 3. Temperature dependence of 2.8 (△) and 4-kG (○) signal amplitudes for constant $\vec{P} \parallel [001]$ = 256 kg/cm^2, $\vec{H} \parallel [1\bar{1}0]$. Solid curve is mean of corresponding data from Fig. 1 scaled as P/T (see text).

Since we observe some line shifts with stress, it is clear that the precision of the previously reported g values[1] was overoptimistic. For example, between 0 and 160 kg/cm^2 the 2.8-kOe line shifts up field by 50 Oe while the 4.0-kOe line shifts down by 75 Oe. Above this stress level no further shift is observable.

In previous work above 4.5 K it was not possible to detect any microwave power saturation of the resonance signals at the standard power level of 20 mW used there and throughout this work. This was tested again with sample 1 at 1.8 and 4.2 K. It was found that there is negligible saturation in lightly stressed samples, but that at high stress, signals at 20 mW do suffer some saturation. For example, 1.8-K signals give about 80% of their unsaturated amplitudes with a stress of 530 kg/cm^2. No shape changes were discernible as a result of this.

An attempt also was made to determine the rate of signal recovery from stress. It was found to take no more than an instrumentally determined 0.2 sec for complete repopulation of the states, even at 1.8 K. Within experimental error, no hysteresis was observed in the EPR signals as stress values were cycled.

Stress || [111]

Stress at this orientation also results in a change in the EPR signals. Smaller transition probabilities, and relaxation effects which will be discussed later, make these data much less precise than those of Fig. 1. It is possible, however, to say that stress has very little effect on the positions of observable lines. The amplitudes of the various components do vary with stress but only the 2.8-kOe line gave usable results. They will be shown later (Fig. 5).

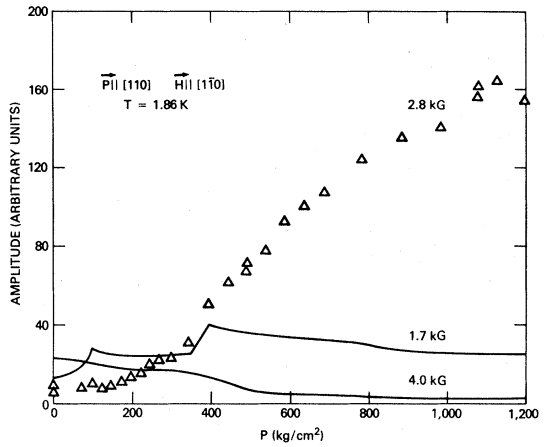

FIG. 4. Variation with stress of signal amplitudes for $\vec{P} \parallel [110]$, $\vec{H} \parallel [1\bar{1}0]$ at 1.86 K. The solid curves represent connected data points.

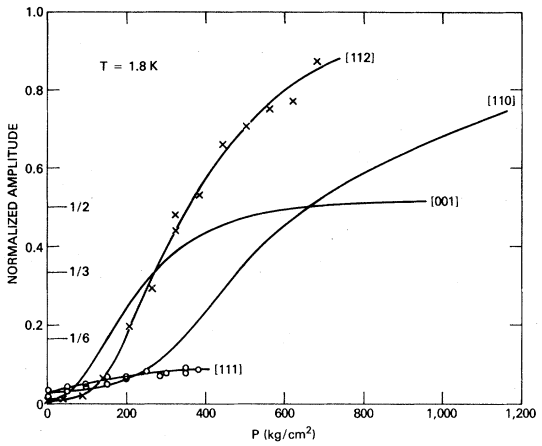

FIG. 5. Stress dependence of the amplitudes of 2.8-kG signals at the four stress orientations used, for $\vec{H} \parallel [1\bar{1}0]$ and at 1.8 K. Data normalized to amplitude of maximum possible signal (see text). Solid lines with the [112] and [111] data are eye aids only. The [001] and [110] curves are taken from Figs. 1 and 4, respectively.

Stress ∥ [110]

Two samples were examined with stress applied along this axis. They are in essential agreement, but only sample 3 which gave stronger signals will be discussed. The variation in signal amplitudes is shown in Fig. 4 for $T = 1.8$ K. In this case it appears that with the levels of stress used, it was not possible to reach a saturated population distribution. For unknown reasons the amplitudes of the 1.7- and 4-kOe signals sometimes showed erratic and irreproducible kinks as the applied stress was changed, although the dominant 2.8-kOe line was well behaved. With stress at this orientation the widths of the 2.8- and 4-kOe lines show some broadening at low stresses. The 1.7-kOe line, which has a rather irregular shape, shows no evident shift under stress. The 4-kOe line also shifts very little, while the 2.8-kOe line shifts −75 Oe in the range 0 to 245 kg/cm^2. Beyond this point a much slower rate of shift persists, but the total shift amounts only to −100 Oe at 960 kg/cm^2 applied.

Sample 3 contains Mn as an additional dopant. Its concentration is sufficient to produce Mn^{2+} signals much larger than those from Cr despite a very great deal of microwave power saturation. The only apparent effect of stress on the complex of six overlapping Mn^{2+} lines[10] is a slight reduction in the amplitudes of individual peaks.

Stress ∥ [112]

The effect of stress on the dominant 2.8-kOe signal amplitude will be shown later (Fig. 5). The other signals are always very small in comparison to the 2.8-kOe signal above 100 kg/cm^2. As with the other orientations, stress affects the resonance linewidths principally in the low-stress regime below 300 kg/cm^2 with the lines narrowing with increasing stress. Very little shift occurs in the position of the 4-kOe line; the 2.8-kOe line is displaced about −50 Oe between 150 and 600 kg/cm^2 and changes little beyond this.

It is useful at this point to put the amplitude data for the stress-favored signals on a common basis for all the directions of applied stress examined. This is done in Fig. 5. Here the data have been normalized to account for the different transition probabilities, numbers of Cr^{3+} centers, and experimental conditions so that a value of unity corresponds to having all Cr^{3+} centers in a sample distorted in the same orientation. (The stress-independent high-stress linewidth was assumed in this normalization.) In making this normalization, it is important to have good values for the total Cr^{3+} concentrations. The values in Table II were obtained using an EPR-optical technique we have developed[11] and are estimated to have accuracies relative to each other of about 20%. If statistical considerations alone governed the curves of Fig. 5, each should start at $\frac{1}{6}$ for zero applied stress. The [110] and [112] stress curves, which have single favored distortions, should approach 1 at high stress, while the [001] and [111] curves with two and three favored distortions should approach $\frac{1}{2}$ and $\frac{1}{3}$, respectively.

DISCUSSION

General

The experimental data given in the preceding section can be summarized as follows:

(1) At 4.2 K and even 1.8 K only weak Cr^{3+} signals are seen in the absence of applied stress.

(2) With applied stress, signals of some centers increase as shown in Fig. 5 and become dominant while those of others decrease or remain relatively weak (Fig. 4).

(3) At high stress the dominant EPR signals have Gaussian shapes with stress-independent widths but show a tendency to broaden and become more nearly Lorentzian at low stress.

(4) The positions of the observed EPR signals show small shifts (50–100 Oe) at low stress but then become stress independent.

(5) There is very little microwave saturation even at 20 mW and 1.8 K, and then only at high-stress levels.

(6) Even at 1.8 K the signals respond to a change in stress in ≤ 0.2 sec.

(7) The centers interact with strains of both E and T_2 symmetry. This is most clearly evident by comparison of the $\vec{P}\parallel[001]$ and $\vec{P}\parallel[110]$ data and Table I.

(8) The data of Figs. 1–3 indicate that the signal amplitudes and widths are functions only of the ratio P/T at least for $\vec{P}\parallel[001]$ where we have sufficiently good data for such an analysis.

The above results argue convincingly that the orthorhombic symmetry of the $Cr^{3+}(3d^3)$ centers are due to Jahn-Teller distortions. Since we observe signals only from centers of C_{2v} symmetry even when we apply large stresses along high-symmetry ([001], [111]) axes, it is clear that the orthorhombic minima in E_a-Q space must be sufficiently deep that their character is not altered by the applied stress. Also the rapidity with which the distortions respond to applied stress definitely rules out associated defects as a possible source of the observed symmetry.

The behavior of the dominant signals at relatively large stress (Fig. 5) is essentially that expected from a Boltzmann distribution over the different distortions whose relative energies are given by Eq. (5). As the stress is reduced, however, the observed normalized amplitudes fall below the value of $\frac{1}{6}$ expected. This reduction in amplitude is clearly related to the increase in width at low stress shown in Figs. 1 and 2. The question then is whether the increased linewidth at low stress is static or dynamic in origin.

If one assumes that the broader linewidth at low stress is due somehow to a static distribution of random strains in the sample and that the state of strain becomes more uniform when the stress-induced strains grow larger than the random ones, one would expect this effect to be temperature independent. As is seen from the P/T scaling observed in Fig. 3, however, one must apply larger stress at higher temperatures to achieve the same reduced linewidth. Also the stress independence of the line positions at high stress makes it difficult to support an explanation in terms of random static strains since a mechanism saturating the effect of strain would then be necessary. The tendency of the lines to become more Lorentzian at low stress also would be unexpected in that case. On the other hand, all these features are in accord with a dynamic explanation of the increased width at low stress. The importance of dynamic processes for Cr^{3+} in GaAs is also indicated by the lack of microwave saturation. An orbital-singlet ground state, such as Cr^{3+} possesses in C_{2v} symmetry, would be expected to exhibit strong microwave saturation at 1.8 K unless there is a dynamically enhanced spin-lattice–relaxation rate.

Our interpretation of these results is that through the application of stress one inhibits rapid reorientation between the well-defined distortion minima on the E_a surface. This is the stress-induced dynamic-to-static transition we referred to earlier. It is possible, of course, for residual strains in the sample to accomplish the same thing but apparently they are much smaller than those intentionally introduced. As we noted earlier[7] in our analysis of the temperature-dependent line broadening of the Cr^{2+} center in GaAs, if the reorientation rate between distortions is less than the splitting of the ground spin state (~200 GHz for Cr^{3+} in GaAs), then there will be a Lorentzian linewidth parameter T_2^{-1} approximately equal to τ^{-1}, the reorientation rate. If the spin-lattice time $T_1 \simeq T_2$ as we expect, one would not anticipate observing a motionally narrowed resonance signal at high temperatures and no such signals have been seen for either Cr^{2+} or Cr^{3+} in GaAs.

Since these dynamic effects play such an important role in the observed behavior of the Cr^{3+} center, in order to be more quantitative in our explanation we must model the center in a way which includes such dynamic effects from the beginning.

Stress model with reorientation

We first consider how such a reorientation process would affect the actual observed linewidths and signal amplitudes. The origin of the constant linewidth at high applied stress is thought to be inhomogeneous broadening by superhyperfine interactions with the neighboring 100% abundant Ga and As nuclear moments. However, the individual spin packets which make up the Gaussian envelope (with derivative width W_G) are taken to have Lorentzian shapes with derivative width $W_L = (2/\gamma\sqrt{3})T_2^{-1} \simeq \gamma^{-1}\tau^{-1}$, where γ is the gyromagnetic ratio. The case of a Gaussian-distributed set of Lorentzian

lines is considered in the Appendix of Ref. 7, where $r \equiv W_L/W_G$ is treated as a parameter. For $0 \leq r \leq 2$ the ratios of the actual derivative linewidth W and amplitude S to those of the pure Gaussian are given there as a function of r. For example, when r exceeds 0.05, the actual amplitude begins to fall significantly below that of the Gaussian and is a factor of 4 smaller for $r = 0.75$. We make explicit use of this variation of W and S with τ^{-1} in our model.

Englman,[12] following Sussmann,[8] gives explicit expressions for the one-phonon-induced transition rates between two potential minima. For the transition from the lower to the upper energy minimum the rate has the form

$$\nu_{lu} = A\,\delta E[\exp(\delta E/kT) - 1]^{-1}, \tag{6}$$

where δE is the energy separation between the two minima and $A = [d(\delta E)/de]^2(4t)^2/\pi\rho\hbar^4c^5$ is dependent on the tunneling matrix element t and the strain sensitivity of δE. Here c is a suitably averaged sound velocity and ρ is the density. We expect the one-phonon process to be dominant at the low temperatures considered here. From detailed balance we have $\nu_{ul} = \nu_{lu}\exp(\delta E/kT)$ in thermal equilibrium.

This result can be generalized to deal with the six minima which occur in the GaAs:Cr^{3+} case. Each possible pair is treated in analogy to the case above. Hence for a given minimum i the frequency of transitions to all other minima is given by

$$\nu_i = \sum_{j(\neq i)} A_{ij}(E_j - E_i)[\exp(E_j - E_i)/kT - 1]^{-1}. \tag{7}$$

Since t vanishes, as mentioned above, for two distortions which have the same cube-edge principal axes, no transitions are induced between the corresponding minima. Thus the Lorentzian width to be associated with the EPR signals from a given distortion can be written as

$$W_{Li} = \tfrac{1}{4}W_0 \sum_j{}' \left(\frac{\delta_{ij}}{kT}\right)\left[\exp\left(\frac{\delta_{ij}}{kT}\right) - 1\right]^{-1}, \tag{8}$$

where $\delta_{ij} = E_i - E_j$. It can be seen that in addition to a functional dependence on $\delta_{ij}/T \propto P/T$ this now has an implicit factor of T in W_0. The prime indicates that one neglects the orthogonal distortion in making the sum. Note that for small δ_{ij}, $W_{Li} \simeq W_0$ so that W_0 is a measure of the Lorentzian broadening when the levels are nearly degenerate.

When stress is applied along any given axis the energies of the various minima are given by Eq. (5) and Table I and hence depend linearly on the local E- and T_2-type strains. This completes the model which, together with Boltzmann statistics, should describe the behavior of the signal amplitudes as a function of temperature and applied stress in terms of the Jahn-Teller parameters b and c and the reorientation parameter W_0.

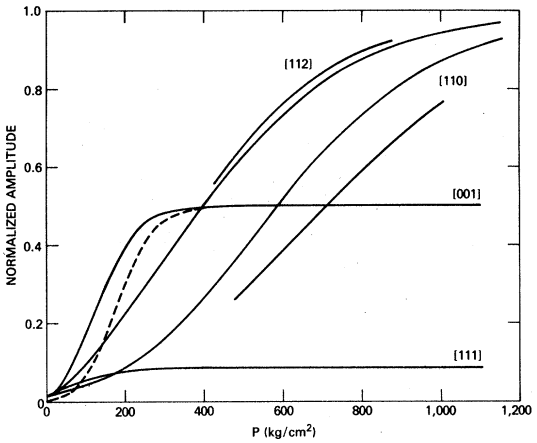

FIG. 6. Computed stress variation of normalized 2.8-kG signal amplitudes based on model in text for 1.8 K. Dashed curve shows effect on [001] curve of raising temperature to 4.2 K. Incomplete curves show effect on [112] and [110] curves of decreasing T_2-mode coupling by 5.4%. The values used are $b/\sqrt{3} = -0.64$ eV/Å, $c = 0.75$ eV/Å, $W_0 = 1.46W_G$.

In Fig. 6 we show the results of such a calculation for the normalized amplitude of the favored 2.8-kOe EPR line for stress along each of the axes studied. These curves are to be compared with the corresponding ones in Fig. 5 and were generated using $W_0/W_G = 1.46$, $T = 1.8$ K, $b/\sqrt{3} = -0.64$ eV/Å, and $c/b = -0.67$. In constructing Fig. 6 the experimental elastic moduli[13] of GaAs, $(s_{11} - s_{12}) = 1.51 \times 10^{-12}$ and $s_{44} = 1.66 \times 10^{-12}$ cm²/dyn, have been used. Since the Gaussian linewidth is about 100 G, the above value of W_0 corresponds to a reorientation time of roughly 0.3 nsec.

Clearly the curves of Fig. 6 describe qualitatively all the principal features of Fig. 5 including the very weak amplitudes at very low stress and the roughly S shaped increase with applied stress. The replica is not exact, however, and we have not been able to find a choice of b, c, and W_0 which improves significantly on that shown here. The value of b is largely set by matching the absolute stress scale, the ratio c/b by the relative rates at which the [110] and [112] curves approach saturation, and W_0 by the ultimate signal amplitude achieved under [111] stress. The values of b and c are not strongly dependent on W_0 since at very large stresses the line broadening is slight. The effect of a 5.4% decrease in $|c/b|$ is indicated by the short sections which parallel the [110] and [112] curves in Fig. 6. Thus this ratio is fixed by the data to about ±5%. The model also predicts the behavior of the energetically disfavored distortions. These results, not presented in detail here,

generally conform well with observation, particularly in showing the persistence of the 1.7-kOe lines for [110] and [111] stress.

To compare the Jahn-Teller coupling of the Cr ($3d^3$) center to E and T_2 distortion modes we need values for κ_E and κ_T. Unfortunately, there is no optical absorption or luminescence data on this center which might give us some direct data. In the absence of that we estimate κ_E and κ_T from the elastic moduli. Proper attention to the definitions of e_θ, f_θ, etc., leads to the following relations for the bulk elastic constants: $\kappa_E = a_0/(s_{11} - s_{12})$ and $\kappa_T = a_0/2s_{44}$. Using[13] $a_0 = 5.651$ Å these give $\kappa_E/\kappa_T = 2.20$ and $\kappa_E = 3.74 \times 10^4$ erg/cm^2. If these values are combined with the c/b ratio -0.67 used to construct Fig. 6, we find that $b^2/\kappa_E \simeq c^2/\kappa_T$ so that the couplings to the E and T_2 modes are nearly "equal" in the sense of O'Brien.[4] Considering the approximations involved in estimating κ_E/κ_T and on the experimental uncertainties inherent in Fig. 5, it would be more accurate to say that the couplings are comparable. O'Brien has shown that the Jahn-Teller reduction factors $K(E)$ and $K(T_2)$ are both 0.4 for the equal case. This reduction helps explain why the random strains which achieve a static JT distortion for the Cr^{2+} center leave the Cr^{3+} center in a "dynamic" state in the same GaAs crystal.

The lowest-order approximations for the equilibrium values of Q_θ and Q_{xy} are $b/\sqrt{3}\kappa_E$ and $-c/\kappa_T$. With the above parameters these correspond to local e_θ and e_{xy} strains of -0.12 and -0.18, respectively. In contrast, the largest external stress-induced strains were only 0.0014 and 0.0007, indeed small perturbations. The large equilibrium values emphasize the likelihood of anharmonic elastic or quadratic Jahn-Teller contributions to the Jahn-Teller energy. Evaluation of Eq. (4) gives a "linear only" estimate $E_{JT} \simeq 2800$ cm^{-1} with a splitting of $\simeq 8500$ cm^{-1} for the Cr($3d^3$) $^4T_1$ ground manifold. In the "equal" case the two excited states are degenerate.[14] We note that this Jahn-Teller splitting is larger than that roughly estimated previously[1] from the spin-Hamiltonian parameters (~5600 cm^{-1}). The difference probably is indicative of the accuracy which either value can claim.

The behavior of the [111] stress signals, which saturate far below the statistically expected amplitude, support the concept that rapid reorientation persists among distortions which remain degenerate in energy under stress. One can construct an alternative reorientation process involving excitation to the real excited states which will mimic the behavior of Figs. 5 and 6 in most respects and it is not possible to rule out such transitions completely. However, in such a process, the lifetime limitation will depend only on the depth of each individual energy minimum so that the normalized [111] stress signal should saturate at its full statistical value of $\frac{1}{3}$.

The absence of complete P/T scaling in our model has the effect of increasing W_0 on going from 1.8 to 4.2 K through the implicit factor of T in Eq. (6). For the [001] case this will result in a shift in the calculated curve of Fig. 6 as indicated by the dashed curve; there will be similar displacements (not shown) of the other parts of the figure. This difference appears somewhat large in comparison with the scatter in the data in Figs. 2 and 3 but is perhaps acceptable in view of the simplifications inherent in the model, particularly that of a stress-independent W_0.

Another aspect of the model is worth noting. The general effect of the coupling between individual distortions is to cause eigenstates of the system to be mixtures of distortion modes whenever these are degenerate in energy. This feature is not changed by allowing some coupling between members of "orthogonal" pairs. It must then be presumed that the separation of such states, as in our [001] and [111] cases, arises from accidental breaking of the degeneracy by random internal strains. Such a contribution also can account for the difference in amplitude of the 2.8- and 4-kG signals for [001] stress. This effect may be at work as well in the [111] case where 1.7-kG lines, with allowance for transitions-probability differences, should behave like the 2.8-kG line but with 0.83 of its intensity. Instead, the 1.7-kG lines are weaker and actually decrease in intensity. This last point may be due to a misalignment of the applied stress, but a further refinement of the model may be necessary. For example, since the 1.7-kG lines remain degenerate in a magnetic field, the effective value of W_0 between such states may be larger than it is between magnetically inequivalent states.

We have no explanation for a splitting we observe in the low-stress 4-kG signal for $\vec{P} \parallel$ [001]. At stresses below 160 kg/cm^2 this line gradually separates into a doublet. At low stresses the internal stresses would have their greatest influence, but we have found no stress condition which will shift the resonance field as high as the upper component of the doublet. Furthermore, since this signal represents a minimum in the resonance g factors, an admixture of distortion states would be expected to raise, not lower, the effective g.

Finally, we note that the existence of fast stress-dependent reorientation at the lowest temperatures used suggests that at such temperatures stress could be applied to tune the reorientation rate for the Cr^{3+} centers to rates observable by ultrasonic means.[15]

SUMMARY

The application of controlled external stress clearly shows the Jahn-Teller nature of the orthorhombic $Cr^{3+}(3d^3)$ center in GaAs:Cr. This stress causes the variously distorted centers to become energetically inequivalent and enhances the relative EPR signal(s) from the favored orientation(s). The data support the idea of well-defined energy minima with orthorhombic symmetry on the E_a vs Q_E, Q_{T_2} surface. As the stress approaches zero, the signal amplitudes generally decrease, the lines broaden and become more nearly Lorentzian, small shifts in line position occur, and there is no microwave saturation even at 1.8 K. This is taken as evidence for "dynamic" behavior involving very rapid ($\tau < 1$ nsec) reorientation between equivalent distortions. Application of stress quenches the reorientation for the favored distortions, thus inducing a "dynamic-to-static" transition. A model which incorporates a stress-dependent reorientation broadening gives a good semiquantitative account of the observed behavior and permits the Jahn-Teller-coupling coefficients for both E and T_2 modes to be estimated. The couplings are found to be "equal" to a good approximation, consistent with the observed C_{2v} symmetry. Certain aspects of the data, such as the rather good P/T scaling of the linewidths and amplitudes as well as an observed line splitting at low stress (all for $\vec{P} \parallel [001]$), remain unexplained.

ACKNOWLEDGMENTS

The samples used were kindly provided by E.M. Swiggard, S.H. Lee, and P.F. Lindquist. This work was supported in part by the Office of Naval Research.

[1] J. J. Krebs and G. H. Stauss, Phys. Rev. B 15, 17 (1977).

[2] For a useful review of the Jahn-Teller effect in EPR see F. S. Ham, in *Electron Paramagnetic Resonance*, edited by S. Geschwind (Plenum, New York, 1972), pp. 1–119.

[3] M. Bacci, A. Ranfagni, M. P. Fontana, and G. Viliani, Phys. Rev. B 11, 3052 (1975); M. Bacci, A. Ranfagni, M. Cetica, and G. Viliani, *ibid.* 12, 5907 (1975).

[4] M. C. M. O'Brien, Phys. Rev. 187, 407 (1969).

[5] U. Öpik and M. H. L. Pryce, Proc. R. Soc. London A 238, 425 (1957).

[6] F. S. Ham, Phys. Rev. 166, 307 (1968).

[7] J. J. Krebs and G. H. Stauss, Phys. Rev. B 20, 795 (1979).

[8] J. A. Sussmann, J. Phys. Chem. Solids 28, 1643 (1967).

[9] I. B. Bersuker and V. Z. Polinger, Zh. Eksp. Teor. Fiz. 66, 2078 (1974) [Sov. Phys.—JETP 39, 1023 (1975)].

[10] R. Bleekrode, J. Dieleman, and H. J. Vegter, Phys. Lett. 2, 355 (1962).

[11] G. S. Stauss, J. J. Krebs, S. H. Lee, and E. M. Swiggard, J. Appl. Phys. 50, 6251 (1979).

[12] R. Englman, *The Jahn-Teller Effect in Molecules and Crystals* (Wiley, London, 1972), p. 192.

[13] R. I. Cottam and G. A. Saunders, J. Phys. C 6, 2105 (1973).

[14] Such a degeneracy is inconsistent with the observed spin-Hamiltonian E/D ratio, given the approximate theoretical expressions used in Ref. 1. Since the other resonance parameters are not fully consistent with these expressions, this discrepancy is not surprising. A possible alternative explanation of an orthorhombic distortion has been raised by A. M. Stoneham and M. Lannoo, J. Phys. Chem. Solids 30, 1769 (1969), based on Jahn-Teller coupling of the ground triplet to another electronically degenerate state which is accidentally nearby. Such a situation would alter the theoretical expressions considerably and may merit further study. Cf. L. A. Hemstreet and J. O. Dimmock, Phys. Rev. B 20, 1527 (1979).

[15] See H. Tokumoto and T. Ishiguro, J. Phys. Soc. Jpn. 46, 84 (1979); 46, 1944(E) (1979).